INSTITUTE OF PHYSICS PUBLISHING SUPERCONDUCTOR SCIENCE AND TECHNOLOGY

Supercond. Sci. Technol. **18** (2005) 776–779 doi:10.1088/0953-2048/18/5/034

Magneto-optical studies of flux penetration in super-hard Nb wire

D P Young[1], M Moldovan[1], P W Adams[1] and R Prozorov[2]

[1] Department of Physics and Astronomy, Louisiana State University, Baton Rouge, LA 70803, USA
[2] Department of Physics and Astronomy, University of South Carolina, Columbia, SC 29208, USA

Received 24 January 2005, in final form 31 March 2005
Published 15 April 2005
Online at stacks.iop.org/SUST/18/776

Abstract

We present a study of the magnetic response of type-II superconductivity in the extreme pinning limit, where screening currents within an order of magnitude of the Ginzburg–Landau depairing critical current density develop upon the application of a magnetic field. We show that this 'super-hard' limit is realized in highly disordered, cold drawn, Nb wire whose magnetization response is characterized by a cascade of Meissner-like phases, each terminated by a catastrophic collapse of the magnetization. Direct magneto-optic measurements of the flux penetration depth in the virgin magnetization branch are in excellent agreement with the exponential model in which $J_c(B) = J_{co}\exp(-B/B_0)$, where $J_{co} \sim 5 \times 10^6$ A cm^{-2} for Nb. The implications for the fundamental limiting hardness of a superconductor are discussed.

In contrast to type-I superconductors, type-II systems support a mixed state consisting of an array of Abrikosov vortex lines [1, 2]. Technologies requiring high current densities and/or high fields typically utilize 'hard' type-II superconductors in which dissipative vortex flow is inhibited by deep vortex pinning centres [3, 4]. Here we explore the fundamental limiting hardness of a superconductor by addressing the thermodynamic, magnetic, and macroscopic quantum characteristics of superconductivity in the presence of pinning forces of sufficient strength to support current densities approaching the Ginzburg–Landau depairing critical current, J_c^{GL} [1]. Using magnetization, magneto-thermal, and magneto-optical probes, we show that this maximum pinning limit [4–6] is well approximated in cold drawn Nb wire, where screening currents of the order of 12% of J_c^{GL} develop upon the application of a magnetic field.

The response of a superconductor to an applied magnetic field in the presence of strong pinning is determined in large degree by the competition between vortex pinning forces and the Lorenz force arising from induced screening currents. Early studies of hard superconductors, such as those of the Nb–Sn, Mo–Re, and Nb–Zr families [7], revealed quantitatively different magnetic properties from those of soft superconductors. In particular, the hard systems exhibited much higher upper critical fields and were much more hysteretic than is typical of soft superconductors. By the early 1960s a number of critical state models of the magnetization response [8] of hard superconductors were developed. The models all assume that a strong pinning system is always in a critical state characterized by a critical current J_c flowing in the regions of flux penetration. In the exponential model [4, 9], for instance,

$$J_c = J_{co}\exp(-B/B_0), \tag{1}$$

where B_0 is a phenomenological characteristic field, and J_{co} is an intrinsic critical current density. The model is most transparent when applied to the virgin magnetization response of a zero-field-cooled superconductor. Solving Maxwell's equation $\mu_0\mathbf{J} = \nabla \times \mathbf{B}$ in a cylindrical geometry of radius R and length $L \gg R$, one finds that upon the application of an external field $H > H_{c1}$ vortices enter from the surface and penetrate to a depth

$$d = d_0[\exp(\mu_0 H/B_0) - 1], \tag{2}$$

where $d_0 = B_0/(\mu_0 J_{co})$ is a characteristic penetration depth which is normally much larger than the London penetration depth λ. Gradients in the vortex density produce Bean currents that flow within this annulus and serve to shield the applied field. If $d < R$ then the induction interior to d is zero ($B = 0$). At sufficiently high fields, however, flux will penetrate to the centre, $d \geqslant R$. In either case, the resulting

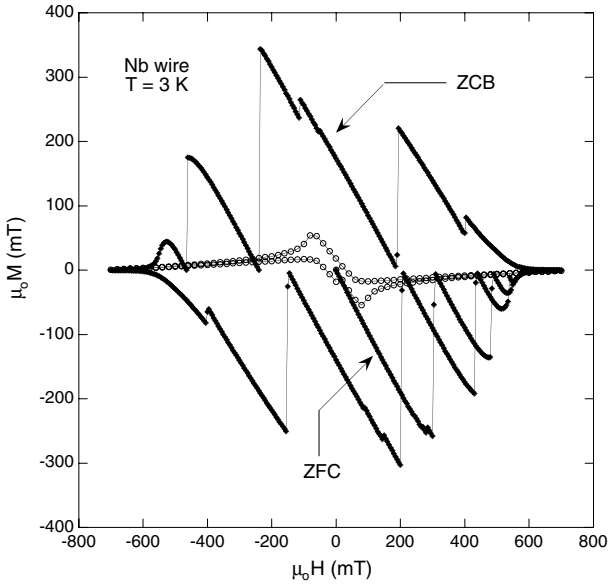

Figure 1. Magnetization of annealed (open symbols) and unannealed (filled symbols) Nb wire as a function of field applied along the wire axis. From a standard analysis of the annealed data we obtain $\mu_0 H_{c1} = 76$ mT, $\mu_0 H_{c2} = 750$ mT, $\mu_0 H_c = 153$ mT, $\lambda = 30$ nm, $\xi = 19$ nm, and $\kappa = 1.6$.

magnetization is simply the volume average $\langle B(\zeta)/\mu_0 - H\rangle$, where $\zeta = R - r$ [8], and $B(\zeta)$ satisfies the boundary conditions $B(0) = \mu_0 H$ and $B(d) = 0$ for $d < R$,

$$B(\zeta) = \begin{cases} B_0 \ln[(\gamma d_0 - \zeta)/d_0] & \zeta < d \\ 0 & \zeta \geqslant d, \end{cases} \tag{3}$$

where $\gamma = \exp(\mu_0 H/B_0)$.

In the context of the above model, the 'hardness' is, in large part, reflected in the magnitude of the intrinsic critical current density J_{co}. One can obtain an estimate of its maximum magnitude, J_{co}^{max}, by considering a rectilinear vortex of length L with a core of radius ξ (the coherence length) that is trapped in a columnar void of length L and radius ξ [11]. By placing its core in the void, the vortex line gains an energy per unit length $U = B_c^2 \pi \xi^2 / 2\mu_0$ with a corresponding pinning force $F_p \approx U/2\xi$. Equating this pinning force with the Lorentz force $F_L = \Phi_0 J_{co}^{max}$, one obtains [15]

$$J_{co}^{max} = \frac{3\sqrt{3}}{32} J_c^{GL} \sim 0.16 J_c^{GL}. \tag{4}$$

In this ultimate hardness limit an applied field can produce extremely high magnetization energies, which in turn lead to well documented thermomagnetic collapses of the magnetization [10, 12–14]. In the present paper, we use magneto-optical (MO) techniques to directly measure the flux penetration depth in the zero-field-cooled state of cold drawn Nb wire in order to extract the two independent parameters of the model, J_{co} and B_0, independent of the magnetization measurements.

Magnetization measurements were made on 1 mm diameter Nb (99.8%) wire obtained from Alpha Aesar. The dc magnetization was measured using a Quantum Design PPMS system utilizing a Faraday extraction technique and a SQUID based MPMS system operating in the standard mode.

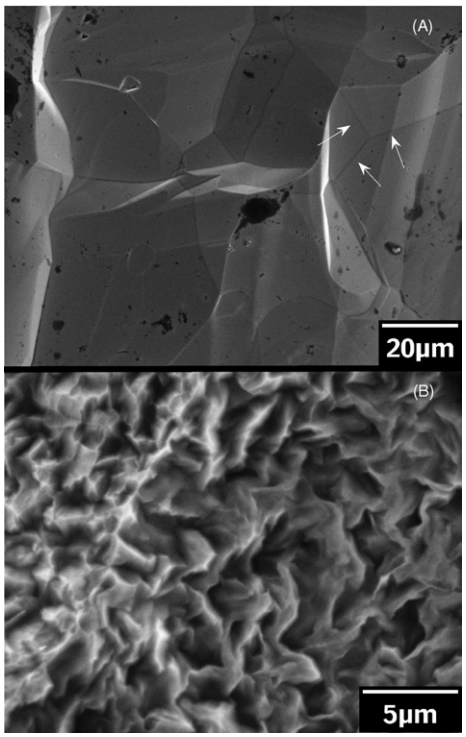

Figure 2. (A) Scanning electron micrographs of the surface of Nb wire after vacuum annealing at 1100 °C for 24 h. The arrows indicate crystalline grain boundaries. (B) Surface of the unannealed wire. The surfaces were prepared by a 5 min etch in a 1:1:2 solution of HNO_3, HF, and HSO_4.

Each system had a base temperature of 1.8 K and maximum field of 9 T. There where no observable differences in the magnetization loops obtained from the two systems. The magnetization samples consisted of wire segments of length ∼6 mm that were sandblasted both to remove the patina and to ensure a uniformly disordered surface. The magnetic flux distribution was imaged via a standard magneto-optical (MO) technique utilizing an in-plane magnetized iron-garnet [16] indicator spatial resolution of ∼5 μm. The MO images were obtained from 0.5 mm thick discs cut and polished from the wire stock. The unannealed Nb wire, from which most of the data were taken, had a 10 K resistivity of 1 $\mu\Omega$ cm and a corresponding mean free path $l_0 \sim 30$ nm. The magnetization and MO measurements were repeated after vacuum annealing the samples at 1100 °C for 24 h.

Shown in figure 1 are the low temperature magnetization curves of an annealed and unannealed Nb wire segment (see figure 2), where the magnetic field was applied along the cylindrical axis. Nb ($T_c = 9.2$ K) is one of only three known type-II elemental superconductors [4], and indeed, the annealed magnetization curves (open symbols) represent classic type-II behaviour. The unannealed curves, however, are profoundly different both in structure and scale, and have several salient features that are worth noting. First, the magnetization energies are extremely high. We have extracted the thermodynamic critical fields from the annealed data by integrating the average magnetization over one half of a field cycle and find that $H_c = 153$ mT. The magnetization of the zero-field-cooled branch, labelled ZFC in figure 1, reaches a maximum value $M_{cr} \sim -2H_c$, which is somewhat

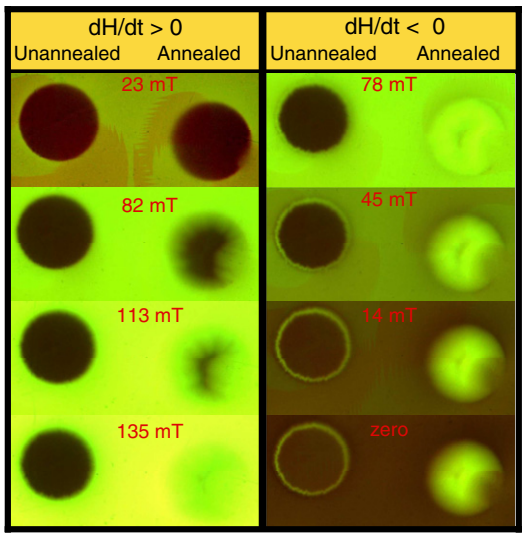

Figure 3. Magneto-optical images of an annealed and unannealed Nb disc at $T = 3$ K with field oriented along the disc axis. The left column corresponds to increasing field and the right to decreasing field. Dark corresponds to zero field.

(This figure is in colour only in the electronic version)

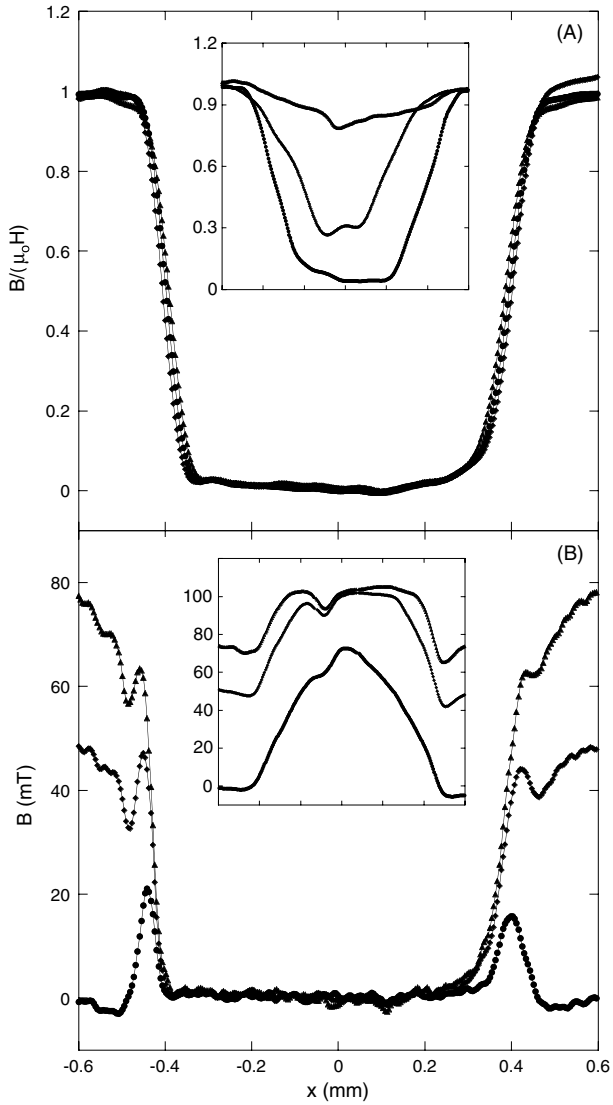

Figure 4. Field profiles obtained from the MO images in figure 3. (A) Increasing field profiles normalized by the applied field, $\mu_0 H = 23$, 82, 113, and 135 mT. (B) Decreasing field profiles after reaching a maximum field of 135 mT. Panel (A) and (B) insets: profiles of the annealed sample at increasing fields of $\mu_0 H = 14$, 45, and 78 mT and decreasing fields of $\mu_0 H = 75$, 45, and 0 mT.

higher than what is typically observed in HTC systems, where $M_{cr} \sim H_c$. Second, upon reaching M_{cr} the Nb magnetization catastrophically collapses to a value that crosses the annealed curve. By attaching miniature thermocouples to the samples we were able to verify that the wires were heated above T_c by the collapse, therefore the re-equilibration occurred along a field-cooled path. As H is increased beyond the first collapse, a series of Meissner-like branches develops: $M^{n+1} = -(H - H^n_{cr})$, where H^n_{cr} is the critical field of the nth collapse. Finally, one might expect that the largest M_{cr} would be observed on the ZFC branch, but in fact, the largest magnetization magnitude develops on the zero-crossing-branch (ZCB) in figure 1.

There is little doubt that microstructural defects induced by the drawing process are producing extremely strong pinning centres in the Nb wires. In figure 2 we show scanning electron micrographs of an unannealed and annealed Nb wire after chemical etching (see figure 2 caption). Etching produced no significant changes in the M–H behaviour, and the micrographs clearly indicate that structural disorder on the scale of microns exists throughout the volume of the unannealed wires. As discussed above, one expects optimal pinning from defects of scale $2\xi \sim 40$ nm. Though submicron structure is evident in figure 2, higher resolution imaging will be needed in order to identify specific pinning centres.

The magnetization collapses in figure 1 are associated with the crossing of a thermomagnetic stability field, B_{sf} [10, 12]. A rough estimate of the ZFC stability field of Nb at $T = 3$ K is given by $B_{sf} \approx \sqrt{\mu_0 c_v (T_c - T)} \sim 250$ mT, which agrees well with the ZFC branch in figure 1, where $c_v \sim 8 \times 10^3$ J m^{-3} K^{-1} is the average volume specific heat of Nb [17] below T_c. Clearly, however, the ZFC branch deviates little from $M = -H$ up to the first collapse, making it difficult to accurately extract J_{co} and B_0 from a fit to the magnetization data or to even establish the appropriateness of the exponential model for this system. To address this issue we present MO images in figure 3 of an Nb disc of length 0.5 mm cut from the 1 mm diameter Nb wire stock. The magnetic field was oriented along the disc axis. Though the discs used in the MO studies were significantly shorter than the wire segments used in the magnetization studies, the MO behaviour of the discs was almost identical to that of the wire segments, after correcting for demagnetization effects. Furthermore, since the disc lengths were much greater than the London penetration depth, $L \sim 10^4\lambda$, we did not need to appeal to thin-film formulations of the Bean model [18].

Note that after ramping to the maximum applied field of the MO system, 135 mT, only a thin shell of vorticity enters the unannealed disc, in stark contrast to the extensive flux penetration in the annealed one. This is most clearly seen in the field profile plots in figure 4. The local minima at $x \sim \pm 0.5$ mm in the 78 and 45 mT induction profiles of figure 4(B) are due to Meissner currents [19]. In figure 5 we plot the penetration depth, d, in the ZFC branch of the

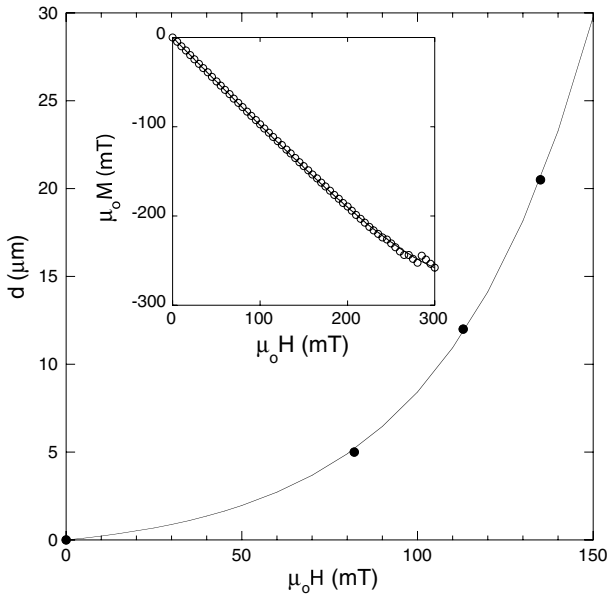

Figure 5. Penetration depth as a function of applied field as determined from the data in figure 4. The solid line is a best fit to equation (2) with $J_{co} = 5.8 \times 10^6$ A cm^{-2} and $B_0 = 62$ mT independently varied. Inset: ZFC branch of the Nb magnetization curve in figure 1. The solid line is a fit to the volume average $\langle (B(\zeta) - \mu_0 H) \rangle$, where $B(\zeta)$ is given by equation (3) and $J_{co} = 5.2 \times 10^6$ A cm^{-2} and $B_0 = 92$ mT were varied.

unannealed Nb disc as a function of H, using the criterion that $B/\mu_0 H = 0.5$ in the profile data of figure 4. It is clear that d is not simply proportional to H. The solid line is a least-squares fit to equation (2) in which d_0 and B_0 were independently varied[3]. Not only is the overall quality of the fit in figure 5 very good, but the extracted values of $J_{co} = 5.8 \times 10^6$ A cm^{-2} and $B_0 = 62$ mT agree very well with values obtain from fits to the ZFC magnetization branch using equations (2) and (3). The ZFC magnetization collapses at $\mu_0 H^1_{cr} \sim 300$ mT, which from equation (2) corresponds to $d \approx 0.25$ mm $\approx R/4$. We note that J_{co} is a factor of 4 higher than reported for the hardest Nb_3Sn tubes in [9], and an order of magnitude higher than the critical currents of cold worked Nb–25% Zr wires of [13]. Indeed, recent measurements of the transport critical current density in Nb films [20] report a depairing critical current $J_c^{GL} \approx 5 \times 10^7$ A cm^{-2} at $T = 3$ K, indicating that $J_{co} \sim 0.12 J_c^{GL}$ and $d_0 \sim 15\lambda$. Interestingly, these critical currents are quite close to the maximum depinning current of equation (4), lending further evidence that the unannealed Nb wire is near its maximum hardness. Similar strong pinning effects have recently been reported in twin boundaries of $YBa_2Cu_3O_{7-\delta}$ [21] and at the edge barriers of MoGe films [22]. Though neither of these systems exhibit significant bulk pinning, they provide compelling evidence that it is possible for pinning potentials to be of sufficient strength so as to accommodate depairing limited screening currents.

In summary, we have correlated magneto-optical measurements of the flux penetration depth with the magnetization behaviour of extremely hard superconducting Nb wires. We find that the virgin magnetic response is very well described by the exponential model with intrinsic critical current densities within an order of magnitude of the depairing critical current. Our analysis suggests that the exponential field dependence of the critical current is, in fact, a fundamental property of the system in this extreme pinning limit. Further studies of the topological characteristics of the pinning centres along with the metallurgical aspects of the drawing process could provide insights into pinning processes in general.

[3] The demagnetization factor of the disc, $N = 1/3$, was taken into account in the determination of B_0.

Acknowledgments

We gratefully acknowledge enlightening discussions with Dana Browne, Milind Kunchur, Ernst Brandt, and Ilya Vekhter. This work was supported by the National Science Foundation under Grant DMR 02-04871.

References

[1] Tinkham M 1996 *Introduction to Superconductivity* (New York: McGraw-Hill)
[2] Abrikosov A A 1957 *JETP* **5** 1174
[3] Wilson M N 1983 *Superconducting Magnets* (Oxford: Clarendon)
[4] Poole C P Jr, Farach H A and Creswick R J 1995 *Superconductivity* (San Diego, CA: Academic)
[5] Schwarz K W 1981 *Phys. Rev. Lett.* **47** 251
[6] Gray K E, Kampwirth R T, Murduck J M and Capone D W II 1988 *Physica* C **152** 445
[7] Blaugher R D and Hulm J K 1962 *Phys. Rev.* **125** 474
[8] Bean C P 1962 *Phys. Rev. Lett.* **8** 250
Bean C P 1964 *Rev. Mod. Phys.* **36** 31
[9] Fietz W A, Beasley M R, Silcox J and Webb W W 1964 *Phys. Rev.* **136** A335
Kumar G R and Chaddah P 1989 *Phys. Rev.* B **39** 4704
[10] Nabialek A, Niewczas M, Dabkowska H, Dabkowska A, Castellan J P and Gaulin B D 2003 *Phys. Rev.* B **67** 0245181
Chababenko V V, Rusakov V F, Piechota S, Nabialek A and Vasiliev S 2002 *Physica* C **369** 82
[11] Brandt E H 1980 *Phys. Lett.* A **77** 484
[12] Wipf S L 1967 *Phys. Rev.* **161** 404
Swartz P S and Bean C P 1968 *J. Appl. Phys.* **39** 4991
[13] Kim Y B, Hempstead C F and Strnad A R 1963 *Phys. Rev.* **129** 528
[14] Brandt E H 1991 *Phys. Rev. Lett.* **67** 2219
[15] Arcos D H and Kunchur M N 2004 Quenched flux motion in magnesium diboride films *Phys. Rev. Lett.* submitted www.physics.sc.edu/kunchur/papers/quenched.pdf
[16] Jooss C, Albrecht J, Kuhn H, Leonhardt S and Kronmueller H 2002 *Rep. Prog. Phys.* **65** 651
Uspenskaya L S *et al* 1997 *Phys. Rev.* B **56** 11979
[17] McConville T and Serin B 1965 *Phys. Rev.* **140** A1169
[18] Mints R G and Brandt E H 1996 *Phys. Rev.* B **54** 12421
[19] Dorosinskii L A *et al* 1993 *Physica* C **206** 360
[20] Yu A, Hesselberth M B S and Aerts J 2004 *Phys. Rev.* B **70** 024510
[21] Maggio-Aprile I, Renner C, Erb A, Walker E and Fischer O 1997 *Nature* **390** 487
[22] Plourde B L T, Van Harlingen D J, Vodolazov D Yu, Besseling R, Hesselberth M B S and Kes P H 2001 *Phys. Rev.* B **64** 014503